J. Fluid Mech. (2014), *vol.* 741, R5, doi:10.1017/jfm.2013.668

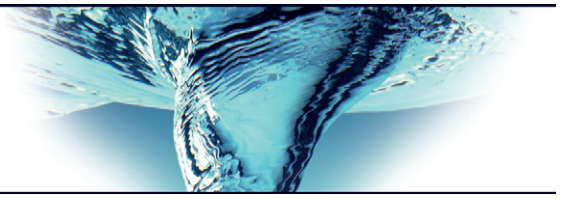

JFM RAPIDS
journals.cambridge.org/rapids

Rotne–Prager–Yamakawa approximation for different-sized particles in application to macromolecular bead models

P. J. Zuk[1], E. Wajnryb[2], K. A. Mizerski[3] and P. Szymczak[1,†]

[1]Institute of Theoretical Physics, Faculty of Physics, University of Warsaw, Hoza 69, 00-681 Warsaw, Poland

[2]Department of Mechanics and Physics of Fluids, Institute of Fundamental and Technological Research, Polish Academy of Sciences, Pawinskiego 5B, 02-106 Warsaw, Poland

[3]Department of Magnetism, Institute of Geophysics, Polish Academy of Sciences, ul. Ksiecia Janusza 64, 01-452 Warsaw, Poland

(Received 23 October 2013; revised 4 December 2013; accepted 13 December 2013)

The Rotne–Prager–Yamakawa (RPY) approximation is a commonly used approach to model the hydrodynamic interactions between small spherical particles suspended in a viscous fluid at a low Reynolds number. However, when the particles overlap, the RPY tensors lose their positive definiteness, which leads to numerical problems in the Brownian dynamics simulations as well as errors in calculations of the hydrodynamic properties of rigid macromolecules using bead modelling. These problems can be avoided by using regularizing corrections to the RPY tensors; so far, however, these corrections have only been derived for equal-sized particles. Here we show how to generalize the RPY approach to the case of overlapping spherical particles of different radii and present the complete set of mobility matrices for such a system. In contrast to previous *ad hoc* approaches, our method relies on the direct integration of force densities over the sphere surfaces and thus automatically provides the correct limiting behaviour of the mobilities for the touching spheres and for a complete overlap, with one sphere immersed in the other one. This approach can then be used to calculate hydrodynamic properties of complex macromolecules using bead models with overlapping, different-sized beads, which we illustrate with an example.

Key words: complex fluids, computational methods, low-Reynolds-number flows, mathematical foundations, suspensions

†Email address for correspondence: piotrek@fuw.edu.pl

1. Introduction

The dynamics of particles suspended in a viscous fluid is governed by the hydrodynamic interactions. Owing to their multi-body and nonlinear nature, hydrodynamic interactions are hard to take into account in their full complexity. Instead, one must resort to various approximations in order to make the computations more tractable. One of the most popular approaches is the Rotne–Prager–Yamakawa (RPY) approximation, based on the following idea. When a force (or torque) is applied to particle i, that particle begins to move, inducing flow in the bulk of the fluid. The effect of this flow on the translational and rotational velocities of another particle (j) is then calculated using Faxen's laws (Kim & Karrila 1991). In that way, one neglects not only the multi-body effects (involving three and more particles) but also the higher-order terms in two-particle interactions (e.g. the impact of the movement of particle j back on particle i). The RPY tensor is by far the most popular method of accounting for hydrodynamic interactions in soft matter modelling (Nägele 2006). In comparison, the very accurate multipole method employs the multiple scattering expansion, which involves summing up the infinite number of reflections of the Stokes flow between all of the particles. The reflected flows include also the higher-order singular and regular solutions of the Stokes equation which are generated during successive reflections. In this framework, the RPY approximation corresponds to a single scattering only, and thus involves pairs of particles and never larger groups.

Notably, the RPY tensor is divergence-free, which considerably simplifies the application of the Brownian dynamics algorithm (Ermak & McCammon 1978). However, when one goes beyond the RPY approximation and includes many-body effects in hydrodynamic interactions, the divergence of the mobility matrix becomes non-zero and needs to be taken into account in Brownian dynamics simulation schemes (Wajnryb, Szymczak & Cichocki 2004). The RPY is a far-field approximation with the corrections decaying at least as fast as the inverse fourth power of the interparticle distances; but it is less accurate at smaller distances. In particular, when the particles overlap, the hydrodynamic tensors calculated based on RPY may become non-positive definite, which causes a problem in the Brownian dynamics simulations where the square root of the mobility matrix is needed. To avoid this problem, one usually uses a regularizing correction for $R_{ij} < a_i + a_j$, which is not singular at $R_{ij} = 0$ and positive definite for all the particle configurations. For the translational components of the mobility matrix of equal-sized spherical particles, such a correction has already been derived by Rotne & Prager (1969). In a recent paper (Wajnryb *et al.* 2013) we have rederived the original RPY tensor using direct integration of force densities over the sphere surfaces and we used this approach to derive the regularizing corrections for rotational and dipolar components of the generalized mobility matrix. Here we show how to use this method to derive the RPY tensors for the particles of different sizes, both non-overlapping and overlapping. The latter case is of particular interest, since the regularizing corrections for unequal overlapping particles have not been derived previously, even for the translational degrees of freedom. Instead, a number of *ad hoc* formulae have been used, such as the Zipper–Durchschlag correction (Zipper & Durchschlag 1997), which lack continuity and do not have the proper limiting behaviour.

The calculation of hydrodynamic tensors for overlapping particles is important for bead–spring models of macromolecules, both rigid and flexible. These models allow for calculation of the dynamic properties of macromolecules, such as the diffusion coefficient and intrinsic viscosity (Kirkwood & Riseman 1948; Bloomfield,

Dalton & Van Holde 1967; Antosiewicz & Porschke 1989; Carrasco & de la Torre 1999). In the case of flexible molecules, one can also track the internal motions and global conformational changes using the Brownian dynamics. The overlapping bead models are particularly often used in coarse-grained models of proteins, in which each amino acid is represented as a number of beads that interact via effective force fields (Tozzini 2005; Clementi 2008; Hills & Brooks 2009). In the simplest version, there is just a single bead per amino acid, usually centred on the position of the C^{α} atom (which is the carbon atom to which the side chain of the amino acid is attached), whereas more complex models involve additional beads representing side chains as well. By tuning the diffusion coefficient of a protein as a whole to the experimental data, Szymczak & Cieplak (2007) found the hydrodynamic radius of the amino acids to be $a \approx 4.1$ Å. Other authors have used similar values of a in their models: e.g. $a = 5.1$ Å (Antosiewicz & Porschke 1989), $a = 3.6$ Å (Hellweg *et al.* 1997), $a = 4.5$ Å (Banachowicz, Gapinski & Patkowski 2000) and $a = 5.3$ Å (Frembgen-Kesner & Elcock 2009). However, since the distance between successive C^{α} atoms along the protein backbone is 3.8 Å, in all of these models some of the beads representing amino acids overlap.

In fact, the non-overlapping bead models ($a < 1.9$ Å) were found to perform unsatisfactorily in protein modelling (de la Torre, Huertas & Carrasco 2000). This reflects the facts that: (i) the interior of the protein is densely packed; (ii) the side chains of amino acids are usually longer than 1.9 Å; and (iii) the protein is covered by a hydration layer of tightly bound water molecules. On the other hand, different amino acids are of different sizes, and a more appropriate protein model would be that of unequal-sized beads. However, the lack of a theoretically sound formulation for hydrodynamic interactions in this case has prevented the wider use of such models (Byron 1997; de la Torre *et al.* 2000). Our paper seeks to fill this gap by showing how to construct the hydrodynamic tensors in the RPY approximation for different-sized overlapping beads. Importantly, the use of this formalism is not limited to proteins only; in principle, any complex shape of a macromolecule would be more faithfully represented by the collection of unequal-sized beads rather than same-sized ones.

We demonstrate that, for rigidly connected overlapping spheres, the hydrodynamic properties calculated using the virtually exact multipole method are surprisingly well reproduced by the corrected RPY model. Additionally, the RPY method is shown to work in the regime where the standard multipole approach cannot be used (corresponding to the situations where the centre of one sphere is inside another).

It is important to realize that the two aforementioned techniques (the multipole method and RPY approximation) are designed with different applications in mind. The multipole technique is a very accurate, although numerically expensive, method of evaluating the hydrodynamic interactions of suspensions of spherical particles. On the other hand, the RPY method is often used for fast simulations of Stokesian and Brownian dynamics of bead-and-spring models of soft-matter systems, where the approximation involved in treating the system as a collection of beads is usually more severe than the fact that not all of the terms in the hydrodynamic interactions have been taken into account.

2. The Rotne–Prager–Yamakawa approximation

We consider a suspension of N spherical particles of different radii a_i, in an incompressible fluid of viscosity η at a low Reynolds number, in a linear shear flow

$$\boldsymbol{v}_\infty(\boldsymbol{r}) = \boldsymbol{K}_\infty \cdot \boldsymbol{r}, \tag{2.1}$$

where $\boldsymbol{K}_\infty$ is the velocity gradient matrix. Owing to the linearity of the Stokes equations, the forces and torques exerted on the fluid by the particles ($\mathcal{F}_j$ and $\mathcal{T}_j$) depend linearly on the translational and rotational velocities of the particles ($\boldsymbol{U}_i$ and $\boldsymbol{\Omega}_i$). This relation defines the friction matrices $\boldsymbol{\zeta}$,

$$\begin{pmatrix} \mathcal{F}_j \\ \mathcal{T}_j \end{pmatrix} = -\sum_i \begin{pmatrix} \boldsymbol{\zeta}_{ji}^{tt} & \boldsymbol{\zeta}_{ji}^{tr} & \boldsymbol{\zeta}_{ji}^{td} \\ \boldsymbol{\zeta}_{ji}^{rt} & \boldsymbol{\zeta}_{ji}^{rr} & \boldsymbol{\zeta}_{ji}^{rd} \end{pmatrix} \cdot \begin{pmatrix} \boldsymbol{v}_\infty(\boldsymbol{R}_i) - \boldsymbol{U}_i \\ \boldsymbol{\omega}_\infty(\boldsymbol{R}_i) - \boldsymbol{\Omega}_i \\ \boldsymbol{E}_\infty \end{pmatrix}, \tag{2.2}$$

where $\boldsymbol{\zeta}^{pq}$ (with $p = t, r$ and $q = t, r, d$) are the Cartesian tensors and the superscripts t, r and d indicate the translational, rotational and dipolar components, respectively. The tensor $\boldsymbol{E}_\infty$ is the symmetric part of $\boldsymbol{K}_\infty$ and $\boldsymbol{\omega}_\infty = \frac{1}{2}\nabla \times \boldsymbol{v}_\infty(\boldsymbol{R}_i) = \frac{1}{2}\boldsymbol{\epsilon} : \boldsymbol{K}_\infty$ is the vorticity of the incident flow. Finally, $\boldsymbol{R}_i$ is the position of particle i. The reciprocal relation giving the velocities of particles moving under external forces and torques in external flow $\boldsymbol{v}_\infty$ is determined by the generalized mobility matrix (Dhont 1996)

$$\begin{pmatrix} \boldsymbol{U}_i \\ \boldsymbol{\Omega}_i \end{pmatrix} = \begin{pmatrix} \boldsymbol{v}_\infty(\boldsymbol{R}_i) \\ \boldsymbol{\omega}_\infty(\boldsymbol{R}_i) \end{pmatrix} + \sum_j \left[\begin{pmatrix} \boldsymbol{\mu}_{ij}^{tt} & \boldsymbol{\mu}_{ij}^{tr} \\ \boldsymbol{\mu}_{ij}^{rt} & \boldsymbol{\mu}_{ij}^{rr} \end{pmatrix} \cdot \begin{pmatrix} \mathcal{F}_j \\ \mathcal{T}_j \end{pmatrix} \right] + \begin{pmatrix} \boldsymbol{C}_i^t \\ \boldsymbol{C}_i^r \end{pmatrix} : \boldsymbol{E}_\infty, \tag{2.3}$$

where the elements of the shear disturbance tensor $\boldsymbol{C}$ are defined as

$$\boldsymbol{C}_i^t = \sum_j \boldsymbol{\mu}_{ij}^{td}, \quad \boldsymbol{C}_i^r = \sum_j \boldsymbol{\mu}_{ij}^{rd}. \tag{2.4a}$$

Finally, the single-particle mobility matrices have the form

$$\boldsymbol{\mu}_{ii}^{tt} = \frac{1}{\zeta_i^{tt}}\mathbf{1}, \quad \boldsymbol{\mu}_{ii}^{rr} = \frac{1}{\zeta_i^{rr}}\mathbf{1}, \quad \boldsymbol{\mu}_{ii}^{tr} = \boldsymbol{\mu}_{ii}^{rt} = \mu_{ii}^{td} = \mu_{ii}^{rd} = 0, \tag{2.5}$$

with friction coefficients for a spherical particle $\zeta_i^{tt} = 6\pi\eta a_i$ and $\zeta_i^{rr} = 8\pi\eta a_i^3$.

Relation (2.3) can be rewritten in a more concise form by introducing the so-called super-vector notation:

$$\begin{pmatrix} \widetilde{\boldsymbol{U}} \\ \widetilde{\boldsymbol{\Omega}} \end{pmatrix} = \begin{pmatrix} \widetilde{\boldsymbol{v}}_\infty \\ \widetilde{\boldsymbol{\omega}}_\infty \end{pmatrix} + \begin{pmatrix} \boldsymbol{\mu}^{tt} & \boldsymbol{\mu}^{tr} \\ \boldsymbol{\mu}^{rt} & \boldsymbol{\mu}^{rr} \end{pmatrix} \cdot \begin{pmatrix} \widetilde{\mathcal{F}} \\ \widetilde{\mathcal{T}} \end{pmatrix} + \begin{pmatrix} \boldsymbol{C}^t \\ \boldsymbol{C}^r \end{pmatrix} : \boldsymbol{E}_\infty. \tag{2.6}$$

Here $\widetilde{\mathcal{F}} = (\mathcal{F}_1, \mathcal{F}_2, \ldots, \mathcal{F}_N)$ is the $3N$-dimensional vector of external forces acting on the particles, and analogously for $\widetilde{\mathcal{T}}$, $\widetilde{\boldsymbol{U}}$ and $\widetilde{\boldsymbol{\Omega}}$. Because of the neglect of inertia, the external forces and torques acting on the particles are equal (and opposite) to those exerted by the fluid on the particles. Finally $\widetilde{\boldsymbol{v}}_\infty = (\boldsymbol{v}_\infty(\boldsymbol{R}_1), \boldsymbol{v}_\infty(\boldsymbol{R}_2), \ldots, \boldsymbol{v}_\infty(\boldsymbol{R}_N))$ and analogously for $\widetilde{\boldsymbol{\omega}}_\infty$. Note that the mobility matrices $\boldsymbol{\mu}^{pq}$ ($p, q = t$ or d) are then $3N \times 3N$ Cartesian tensors. Finally, the whole $6N \times 6N$ matrix in (2.6) comprising $\boldsymbol{\mu}^{tt}$, $\boldsymbol{\mu}^{tr}$, $\boldsymbol{\mu}^{rt}$ and $\boldsymbol{\mu}^{rr}$ is called the N-particle mobility matrix.

In order to make the subsequent analysis more concise, we also introduce the tensors (Wajnryb *et al.* 2013)

$$\boldsymbol{w}_i^t(\boldsymbol{r}) = \frac{1}{4\pi a_i^2}\mathbf{1}\,\delta(\rho_i - a_i), \quad \boldsymbol{w}_i^r(\boldsymbol{r}) = \frac{3}{8\pi a_i^3}\,\boldsymbol{\epsilon}\cdot\hat{\boldsymbol{\rho}}_i\,\delta(\rho_i - a_i), \tag{2.7}$$

where $\boldsymbol{\rho}_j = \boldsymbol{r} - \boldsymbol{R}_j$ is the distance from the centre of sphere j and $[\boldsymbol{\epsilon} \cdot \hat{\boldsymbol{\rho}}_j]_{\alpha\beta} = \epsilon_{\alpha\beta\gamma}[\hat{\boldsymbol{\rho}}_j]_\gamma$. The above tensors multiplied by force $\boldsymbol{w}^t \cdot \boldsymbol{\mathcal{F}}$ and torque $\boldsymbol{w}^r \cdot \boldsymbol{\mathcal{T}}$ have the interpretation of surface force densities on the surface of the sphere due to the force and torque acting on the sphere. Using this notation, the RPY tensor can be conveniently expressed as (Wajnryb *et al.* 2013)

$$\boldsymbol{\mu}_{ij}^{pq} = \langle \boldsymbol{w}_i^p | \boldsymbol{T}_0 | \boldsymbol{w}_j^q \rangle = \iint \mathrm{d}\boldsymbol{r}' \, \mathrm{d}\boldsymbol{r}'' \, [\boldsymbol{w}_i^p(\boldsymbol{r}')]^{\mathrm{T}} \cdot \boldsymbol{T}_0(\boldsymbol{r}', \boldsymbol{r}'') \cdot \boldsymbol{w}_j^q(\boldsymbol{r}''), \tag{2.8}$$

with $p, q = r, t$ and superscript T denoting tensor transposition. In the above, $\boldsymbol{T}_0(\boldsymbol{r}', \boldsymbol{r}'')$ is the Green's function for the Stokes flow given by the Oseen tensor (Kim & Karrila 1991)

$$\boldsymbol{T}_0(\boldsymbol{r}) = \frac{1}{8\pi\eta r}(\boldsymbol{1} + \hat{\boldsymbol{r}}\hat{\boldsymbol{r}}). \tag{2.9}$$

In an analogous manner, one can express the elements of the shear disturbance tensor. First, one observes that the contribution to the surface force density due to the straining fluid motion is equal to $3\eta\delta(\rho_j - a_j)\boldsymbol{E}_\infty \cdot \hat{\boldsymbol{\rho}}_j$, which defines the additional tensor $\boldsymbol{w}^c(\boldsymbol{r})$ by

$$\boldsymbol{w}^c(\boldsymbol{r}) : \boldsymbol{E}_\infty = 3\eta\delta(\rho_j - a_j)\boldsymbol{E}_\infty \cdot \hat{\boldsymbol{\rho}}_j. \tag{2.10}$$

Next, in analogy to (2.8), for the dipolar components of the mobility matrix one gets

$$\boldsymbol{\mu}_{ij}^{td} : \boldsymbol{E}_\infty = \langle \boldsymbol{w}_i^t | \boldsymbol{T}_0 | \boldsymbol{w}_j^c \rangle : \boldsymbol{E}_\infty \tag{2.11}$$

and

$$\boldsymbol{\mu}_{ij}^{rd} : \boldsymbol{E}_\infty = \langle \boldsymbol{w}_i^r | \boldsymbol{T}_0 | \boldsymbol{w}_j^c \rangle : \boldsymbol{E}_\infty. \tag{2.12}$$

3. The explicit form of RPY tensors

Below, we present the analytical expressions for the full set of mobility matrices defined by (2.8)–(2.12). In the following formulae $\boldsymbol{R}_{ij} = \boldsymbol{R}_i - \boldsymbol{R}_j$ is the interparticle distance, $a_>$ ($a_<$) denotes the radius of the larger (smaller) particle in the pair i, j, and $\Theta(x)$ is the Heaviside function.

The integration of (2.8) gives the following form of the translational–translational mobility matrix:

$$\boldsymbol{\mu}_{ij}^{tt} = \begin{cases} \left(\boldsymbol{1} + \dfrac{a_i^2 + a_j^2}{6}\nabla^2\right)\boldsymbol{T}_0(\boldsymbol{R}_{ij}) \\ \quad = \dfrac{1}{8\pi\eta R_{ij}}\left[\left(1 + \dfrac{a_i^2 + a_j^2}{3R_{ij}^2}\right)\boldsymbol{1} + \left(1 - \dfrac{a_i^2 + a_j^2}{R_{ij}^2}\right)\hat{\boldsymbol{R}}_{ij}\hat{\boldsymbol{R}}_{ij}\right], \quad a_i + a_j < R_{ij}, \\ \dfrac{1}{6\pi\eta a_i a_j}\left[\dfrac{16R_{ij}^3(a_i + a_j) - ((a_i - a_j)^2 + 3R_{ij}^2)^2}{32R_{ij}^3}\boldsymbol{1}\right. \\ \quad \left. + \dfrac{3((a_i - a_j)^2 - R_{ij}^2)^2}{32R_{ij}^3}\hat{\boldsymbol{R}}_{ij}\hat{\boldsymbol{R}}_{ij}\right], \quad a_> - a_< < R_{ij} \leqslant a_i + a_j, \\ \dfrac{1}{6\pi\eta a_>}\boldsymbol{1} = \dfrac{1}{\zeta_>^{tt}}\boldsymbol{1}, \quad R_{ij} \leqslant a_> - a_<, \end{cases} \tag{3.1}$$

whereas the rotational–rotational mobility matrix is given by

$$\boldsymbol{\mu}^{rr}_{ij} = \begin{cases} -\dfrac{1}{4}\nabla^2 \boldsymbol{T}_0(\boldsymbol{R}_{ij}) = \dfrac{1}{16\pi\eta R^3_{ij}}(3\hat{\boldsymbol{R}}_{ij}\hat{\boldsymbol{R}}_{ij} - \mathbf{1}), & a_i + a_j < R_{ij}, \\ \dfrac{1}{8\pi\eta a_i^3 a_j^3}(\mathscr{A}\mathbf{1} + \mathscr{B}\hat{\boldsymbol{R}}_{ij}\hat{\boldsymbol{R}}_{ij}), & a_> - a_< < R_{ij} \leqslant a_i + a_j, \\ \frac{1}{8\pi\eta a_>^3}\mathbf{1} = \frac{1}{\zeta^{rr}_>}\mathbf{1}, & R_{ij} \leqslant a_> - a_<, \end{cases} \tag{3.2}$$

with

$$\mathscr{A} = \frac{5R^6_{ij} - 27R^4_{ij}(a_i^2 + a_j^2) + 32R^3_{ij}(a_i^3 + a_j^3) - 9R^2_{ij}(a_i^2 - a_j^2)^2 - (a_i - a_j)^4(a_i^2 + 4a_j a_i + a_j^2)}{64R^3_{ij}} \tag{3.3}$$

and

$$\mathscr{B} = \frac{3((a_i - a_j)^2 - R^2_{ij})^2(a_i^2 + 4a_j a_i + a_j^2 - R^2_{ij})}{64R^3_{ij}}. \tag{3.4}$$

The rotational–translational part of the mobility matrix simply reads

$$\boldsymbol{\mu}^{rt}_{ij} = \begin{cases} \dfrac{1}{2}\boldsymbol{\nabla} \times \left(\mathbf{1} + \dfrac{a_j^2}{6}\nabla^2\right)\boldsymbol{T}_0(\boldsymbol{R}_{ij}) = \dfrac{1}{2}\boldsymbol{\nabla} \times \boldsymbol{T}_0(\boldsymbol{R}_{ij}) = \dfrac{1}{8\pi\eta R^2_{ij}}\boldsymbol{\epsilon} \cdot \hat{\boldsymbol{R}}_{ij}, & a_i + a_j < R_{ij}, \\ \dfrac{1}{16\pi\eta a_i^3 a_j}\dfrac{(a_i - a_j + R_{ij})^2(a_j^2 + 2a_j(a_i + R_{ij}) - 3(a_i - R_{ij})^2)}{8R^2_{ij}}\boldsymbol{\epsilon} \cdot \hat{\boldsymbol{R}}_{ij}, & \\ \quad a_> - a_< < R_{ij} \leqslant a_i + a_j, & \\ \theta(a_i - a_j)\frac{R_{ij}}{\zeta^{rr}_i}\boldsymbol{\epsilon} \cdot \hat{\boldsymbol{R}}_{ij}, \quad R_{ij} \leqslant a_> - a_<. & \end{cases} \tag{3.5}$$

Owing to the symmetry (Kim & Karrila 1991), the translational–rotational mobility matrix is of the same form as $\boldsymbol{\mu}^{rt}_{ij}$ but with interchanged a_i and a_j (note that in equation (3.16) of Wajnryb *et al.* (2013) it was erroneously stated that $\boldsymbol{\mu}^{rt}_{ij}$ is the transpose of $\boldsymbol{\mu}^{tr}_{ij}$).

Finally, the dipolar components of the mobility matrix are of the form

$$\boldsymbol{\mu}^{td}_{ij} = \begin{cases} \dfrac{5}{6}a_j\left[-\dfrac{2(5a_i^2a_j^2 + 3a_j^4)}{5R^4_{ij}}\mathbf{1}\hat{\boldsymbol{R}}_{ij} + \dfrac{a_j^2(5a_i^2 + 3a_j^2 - 3R^2_{ij})}{R^4_{ij}}\hat{\boldsymbol{R}}_{ij}\hat{\boldsymbol{R}}_{ij}\hat{\boldsymbol{R}}_{ij}\right], & a_i + a_j < R_{ij}, \\ \dfrac{5}{6}a_j[\mathscr{C}\mathbf{1}\hat{\boldsymbol{R}}_{ij} + \mathscr{D}\hat{\boldsymbol{R}}_{ij}\hat{\boldsymbol{R}}_{ij}\hat{\boldsymbol{R}}_{ij}], \quad a_> - a_< < R_{ij} \leqslant a_i + a_j, & \\ -\theta(a_j - a_i)R_{ij}\mathbf{1}\hat{\boldsymbol{R}}_{ij}, \quad R_{ij} \leqslant a_> - a_< & \end{cases} \tag{3.6}$$

with

$$\mathscr{C} = \frac{10R^6_{ij} - 24a_iR^5_{ij} - 15R^4_{ij}(a_j^2 - a_i^2) + (a_j - a_i)^5(a_i + 5a_j)}{40a_ia_jR^4_{ij}}, \tag{3.7}$$

$$\mathscr{D} = \frac{((a_i - a_j)^2 - R^2_{ij})^2((a_i - a_j)(a_i + 5a_j) - R^2_{ij})}{16a_ia_jR^4_{ij}} \tag{3.8}$$

and

$$\boldsymbol{\mu}_{ij}^{rd} = \begin{cases} -\dfrac{5}{2}\left[\dfrac{a_j}{R_{ij}}\right]^3 (\boldsymbol{\epsilon}\cdot\hat{\boldsymbol{R}}_{ij})\hat{\boldsymbol{R}}_{ij}, & a_i + a_j < R_{ij}, \\ -\dfrac{5}{3a_i^3}\mathscr{B}(\boldsymbol{\epsilon}\cdot\hat{\boldsymbol{R}}_{ij})\hat{\boldsymbol{R}}_{ij}, & a_> - a_< < R_{ij} \leqslant a_i + a_j, \\ 0, & R_{ij} \leqslant a_> - a_<, \end{cases} \tag{3.9}$$

where $[\mathbf{1}\hat{\boldsymbol{R}}_{ij}]_{\alpha\beta\gamma} = \delta_{\alpha\beta}[\hat{\boldsymbol{R}}_{ij}]_\gamma$. Several remarks are in order here. First, for non-overlapping particles, the integrals defined in (2.8) can be conveniently expressed in terms of the differential operators acting on $\boldsymbol{T}_0$, as detailed in the formulae (3.1)–(3.5) (upper row). For the dipolar components, the analogous formulae read

$$\boldsymbol{\mu}^{td} : \boldsymbol{E}_\infty = \frac{20}{3}\pi\eta a_j^3 \left\{ \left[\left(1 + \frac{5a_i^2 + 3a_j^2}{30}\nabla^2 \right) \boldsymbol{T}_0(\boldsymbol{R}_{ij}) \right] \overleftarrow{\nabla} \right\} : \boldsymbol{E}_\infty \tag{3.10}$$

and

$$\boldsymbol{\mu}^{rd} : \boldsymbol{E}_\infty = \frac{10}{3}\pi\eta a_j^3 \{ [\nabla \times \boldsymbol{T}_0(\boldsymbol{R}_{ij})] \overleftarrow{\nabla} \} : \boldsymbol{E}_\infty, \tag{3.11}$$

where ∇ is a differential operator with respect to R_{ij} and $[\boldsymbol{T}_0(\boldsymbol{R}_{ij})\overleftarrow{\nabla}]_{\alpha\beta\gamma} = \partial_\gamma T_{0\,\alpha\beta}(\boldsymbol{R}_{ij})$. Note that $\boldsymbol{\mu}^{td}$ and $\boldsymbol{\mu}^{rd}$ are not determined uniquely, since they define only the symmetric and traceless parts of the mobility matrix. Given this freedom, in (3.6)–(3.9) we write the matrices in the simplest algebraic form, following the convention of Wajnryb *et al.* (2013).

Next, the self-mobilities of the particles in the RPY approximation can be recovered by taking the limit $R_{ij} \to 0$ in (3.1)–(3.9) and they read (for $a_i \geqslant a_j$)

$$\boldsymbol{\mu}_{ii}^{tt} = \lim_{R_{ij}\to 0} \boldsymbol{\mu}_{ij}^{tt} = \frac{1}{\zeta_i^{tt}}\mathbf{1}, \quad \boldsymbol{\mu}_{ii}^{rr} = \lim_{R_{ij}\to 0} \boldsymbol{\mu}_{ij}^{rr} = \frac{1}{\zeta_i^{rr}}\mathbf{1}, \tag{3.12}$$

whereas

$$\boldsymbol{\mu}_{ii}^{tr} = \mu_{ii}^{rt} = \boldsymbol{\mu}_{ii}^{td} = \boldsymbol{\mu}_{ii}^{rd} = 0. \tag{3.13}$$

Note that the above correspond simply to the single-particle mobilities, since within the RPY approximation the hydrodynamic effects do not enter at this level.

Importantly, the formulae (3.1)–(3.9) reproduce the single-particle mobilities also in the case when the smaller sphere is completely immersed in the larger one. This is to be expected, since in such a case only the external sphere interacts hydrodynamically with the outside world. Note, however, that the phenomenological formulae proposed for the RPY tensors for unequal overlapping spheres (Zipper & Durchschlag 1997; Carrasco, de la Torre & Zipper 1999; Arya, Zhang & Schlick 2006) do not have this property. These issues are discussed in more detail in the next section.

Additionally, one notes that there is no simple correspondence between the RPY formulae for the equal-sized spheres and those for different-sized ones. The notable exception is the translational part of the mobility matrix for non-overlapping particles, which can be obtained from the corresponding formulae for identical spheres by the substitution $a \to [(a_i^2 + a_j^2)/2]^{1/2}$, as already noted by de la Torre & Bloomfield (1977). Unfortunately, such a simple mapping ceases to work as soon as the particles begin to overlap.

Finally, let us stress that the RPY approximation can be generalized to any boundary conditions and corresponding propagators (e.g. in the vicinity of a wall or in periodic boundary conditions), as detailed in (Wajnryb *et al.* 2013). Importantly, the regularizing corrections (corresponding to the extra terms that need to be added to the RPY tensors derived for the non-overlapping case to obtain those for overlapping particles) turn out to be independent of the specific form of the propagator. Thus one can use the above-derived result to construct the RPY approximation for unequal particles with different conditions at the boundaries of the system.

4. Other forms of RPY tensors for overlapping spheres

Several ansätze have previously been proposed in the literature to account for the different sphere radii in RPY tensors. All of them have employed the original RPY formulae for equal spheres, replacing the sphere radius by an effective radius a_{eff}, defined as some function of a_i and a_j. Arguably, the most popular is the ansatz due to Zipper & Durchschlag (1997), where

$$a_{eff} = [(a_i^3 + a_j^3)/2]^{1/3}, \tag{4.1}$$

motivated by the fact that in this case the volume of the two spheres of radius a_{eff} is the same as that of the pair a_i and a_j. Such an effective radius is then inserted into the RPY formula for overlapping equal-sized spheres, i.e. (according to (3.1))

$$\boldsymbol{\mu}_{ij}^{tt} = \frac{1}{6\pi\eta a_{eff}} \left[\left(1 - \frac{9R_{ij}}{32a_{eff}} \right) \mathbf{1} + \frac{3R_{ij}}{32a_{eff}} \hat{\boldsymbol{R}}_{ij}\hat{\boldsymbol{R}}_{ij} \right], \quad R_{ij} < a_i + a_j, \tag{4.2}$$

whereas for the non-overlapping spheres the formula (3.1) (upper row) is used, i.e.

$$\boldsymbol{\mu}_{ij}^{tt} = \frac{1}{8\pi\eta R_{ij}} \left[\left(1 + \frac{a_i^2 + a_j^2}{3R_{ij}^2} \right) \mathbf{1} + \left(1 - \frac{a_i^2 + a_j^2}{R_{ij}^2} \right) \hat{\boldsymbol{R}}_{ij}\hat{\boldsymbol{R}}_{ij} \right], \quad R_{ij} > a_i + a_j. \tag{4.3}$$

On the other hand, Carrasco *et al.* (1999) have analysed the model in which a_{eff} in the overlapping region is a simple arithmetic mean of a_i and a_j, i.e.

$$a_{eff} = (a_i + a_j)/2, \tag{4.4}$$

whereas, in the non-overlapping region, (4.3) is again used. Finally, Arya *et al.* (2006) have proposed to use

$$a_{eff} = [(a_i^2 + a_j^2)/2]^{1/2}, \tag{4.5}$$

which reproduces the correct formula for the translational mobility matrix for non-overlapping spheres. Below, we analyse the predictions of these models and compare them with that of the previously derived (3.1)–(3.9).

As an example, let us calculate the translational mobility of a pair of particles with $a_2 = a_1/2$ as a function of the distance between their centres. Owing to the symmetry of the problem, the mobility tensor $\boldsymbol{\mu}_{12}^{tt}$ is then of the form

$$\boldsymbol{\mu}_{12}^{tt} = \mu_{\parallel}(R_{12})\hat{R}_{12}\hat{R}_{12} + \mu_{\perp}(R_{12})(\mathbf{1} - \hat{R}_{12}\hat{R}_{12}) \tag{4.6}$$

with the components $\mu_{\parallel}(R_{12})$ and $\mu_{\perp}(R_{12})$ presented in figure 1 for a number of different mobility models:

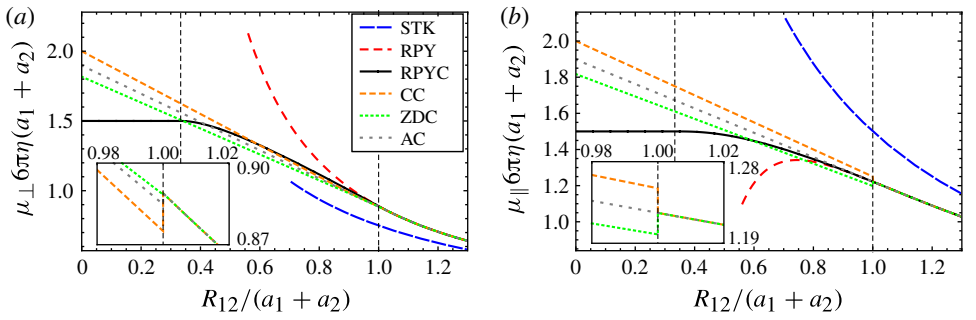

FIGURE 1. The mobility coefficients (*a*) $\mu_\perp$ and (*b*) $\mu_\parallel$ as defined in (4.6) for a system of two overlapping particles with $a_2 = a_1/2$. The dashed vertical lines mark the point of touching ($R_{12}/(a_1+a_2) = 1$) and the distance at which the smaller sphere becomes immersed in the larger one ($R_{12}/(a_1+a_2) = 1/3$). The inset shows the discontinuity of ZDC, AC and CC formulae at $R_{12} = a_1 + a_2$.

(i) STK = the Stokeslet model, with the mobility matrix given by

$$\boldsymbol{\mu}^{tt}_{ij} = \frac{1}{8\pi\eta R_{ij}}(\mathbf{1} + \hat{\boldsymbol{R}}_{ij}\hat{\boldsymbol{R}}_{ij}),\ i \neq j, \quad \boldsymbol{\mu}^{tt}_{ii} = \frac{1}{\zeta^{tt}}\mathbf{1}; \tag{4.7}$$

(ii) RPY = the Rotne–Prager–Yamakawa model without the regularizing correction, which corresponds to using the upper formula in (3.1) over the entire distance range;

(iii) RPYC = the RPY model with the regularizing correction, following the full formula (3.1);

(iv) ZDC = the RPY model with the Zipper–Durchschlag correction, see (4.1);

(v) CC = the RPY model with the correction by Carrasco *et al.* (1999), see (4.4);

(vi) AC = the RPY model with the correction by Arya *et al.* (2006), see (4.5).

Importantly, in figure 1 we plot only the values that correspond to the positive definite 6×6 mobility matrix $\boldsymbol{\mu}^{tt}$ defined by the relation analogous to (2.6). For small interparticle distances, the Stokeslet model produces a non-positive definite matrix, a fact already recognized by Zwanzig, Kiefer & Weiss (1968). An explicit calculation of the determinant of $\boldsymbol{\mu}^{tt}$ shows that it loses its positive definiteness at $R^\star_{12} = 3\sqrt{a_1 a_2}/2$, which for $a_2 = a_1/2$ corresponds to $R^\star_{12}/(a_1+a_2) = 1/\sqrt{2}$, as indeed observed in figure 1. The uncorrected Rotne–Prager model also loses its positive definiteness as the distance between the centres decreases. This time an explicit calculation shows that the threshold value is

$$R^\star_{12} = \tfrac{1}{4}\sqrt{a_1 a_2}\{1 + [f(a_1/a_2)]^{1/3} + [f(a_1/a_2)]^{-1/3}\} \tag{4.8}$$

with

$$f(x) = 1 + 8/x + 8x + 4\sqrt{(1+x^2)(4+x+4x^2)/x^2}. \tag{4.9}$$

For the case at hand, this corresponds to $R^\star_{12}/(a_1+a_2) \approx 0.56$. On the other hand, the corrected models remain positive definite in the entire range of interparticle distances, which was in fact the main reason for their introduction. It needs to be stressed, however, that there is no formal proof that the *ad hoc* models (ZDC, CC and AC) will give positive definite mobility for a general configuration of N particles. Contrastingly,

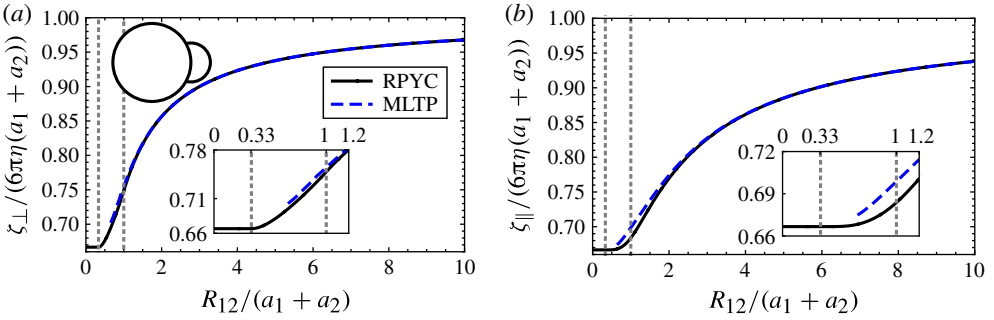

FIGURE 2. The friction coefficients for a snowman-shaped particle comprising two rigidly connected, overlapping spheres with $a_2 = a_1/2$. The panels present the (*a*) transverse friction coefficient $\zeta_\perp$ and (*b*) longitudinal friction coefficient $\zeta_\parallel$ calculated using the RPYC formulae (solid) and the multipole expansion (dashed). The inset shows the magnification of the small R_{12} region.

the RPYC model derived here is positive definite by construction, as it arises from the action of a positive definite operator T_0 on the vectors $\boldsymbol{w}^q$ (cf. (2.8)–(2.12); see also the discussion in Cichocki *et al.* (2000) and Wajnryb *et al.* (2013)).

The analysis of figure 1 shows further that the *ad hoc* models are not continuous at the point of touching, i.e. $a_1 + a_2 = R_{12}$. Such a discontinuity in mobility, albeit small, can lead to numerical artifacts in the Brownian dynamics simulations. In particular, it will affect the resulting shape of the pair distribution function of close particles. An additional negative aspect of the *ad hoc* corrections is their behaviour in the complete overlap region, i.e. when $R_{12} < a_> - a_<$. As already mentioned, the mobility matrices in this region should become independent of R_{12} and reduce to those of the larger (external) particle. Such a behaviour is indeed observed for RPYC tensors, but not in the case of other corrections.

5. Bead models of macromolecules

The overlapping bead models can be used for the calculation of hydrodynamic properties of complex-shaped macromolecules, both rigid and flexible. To illustrate this, we consider a simple example of a snowman-like molecule, formed by two rigidly connected overlapping particles of radii a_1 and $a_2 = a_1/2$. The recent advent of microassembly techniques allows such structures to be relatively easily fabricated (Duguet *et al.* 2011). Figure 2 presents the longitudinal and transverse friction coefficients for such a snowman, defined in analogy to (4.6). These are obtained by inverting the N-particle mobility matrix of (2.6) and then projecting the resulting friction matrix on the rigid-body motion of the snowman as a whole. This is compared with the friction coefficients calculated using the (virtually) exact multipole series expansion method (MLTP) (Cichocki *et al.* 1994; Zurita-Gotor, Bławzdziewicz & Wajnryb 2007).

The data presented in figure 2 show that, even though the RPY approach is formally a far-field expansion, it works surprisingly well also for very small distances between the particles, including the case of overlap. The transverse component is underestimated by the RPYC approximation by no more than $\sim 1\,\%$, whereas the longitudinal component is underestimated by no more than $\sim 2\,\%$. Such a good

accuracy of RPY tensors is due to the fact that the rigid connection between the particles removes the lubrication singularities that normally dominate the hydrodynamic interactions between close particles. This leads to a satisfactory performance of the bead models in which hydrodynamic interactions are accounted for on the RPY level.

Another feature that can be noted in figure 2 is that the multipole results are plotted down to $R_{12}/(a_1 + a_2) = 2/3$ only. This is not coincidental, but a manifestation of a fundamental property of the displacement theorem (Felderhof & Jones 1989), by means of which one expands the singular flows generated by one sphere into regular flows about the centre of another sphere in the multipole method. Namely, when the two spheres are so close that the centre of the smaller one gets inside the larger one, the aforementioned expansion is no longer convergent and the multipole method ceases to work. For $a_2 = a_1/2$ this corresponds to the dimensionless distance of $R_{12}/(a_1 + a_2) = 2/3$, at which the lines in figure 2 terminate. The RPYC method is not limited by this issue, and produces continuous results for arbitrary overlapping, with correct limiting behaviour when one sphere is completely immersed in the other.

Importantly, the RPYC approximation can also be used to track the motion of overlapping spheres that are not rigidly connected, a case that the multipole method cannot handle, again because of the lack of convergence. The physical interpretation of the RPYC results in this case is, however, more problematic than in the case of rigid molecules, since the RPY approximation neglects the lubrication effects, which strongly hinder the normal relative motion of the particle pair as the gap between the sphere surfaces goes to zero. Nevertheless, the overlapping bead models based on the RPY approximation do seem to work adequately for flexible molecules, e.g. proteins (Frembgen-Kesner & Elcock 2009; Szymczak & Cieplak 2011). This is possibly because the individual amino acids behave more like rough, porous objects than smooth impermeable spheres, and thus the lubrication forces are expected to play a less important role there. Also, the steric forces involved in these models limit the amount of relative normal motion of neighbouring particles.

6. Concluding remarks

Reformulation of the RPY approximation using the integral formalism (equations (2.8)–(2.12)) derived in Wajnryb *et al.* (2013) has been extended here to the case of spherical particles of different radii. This has led to several results which, to our knowledge, have not been derived so far. In particular, we have found the explicit form of the dipolar components of the mobility matrix (3.6) and (3.9), needed in order to track the dynamics of the system under shear flow. Additionally, we have derived expressions for all the components of the mobility matrix for overlapping particles, which is needed in both the Brownian dynamics simulations (Długosz, Zieliński & Trylska 2011; Geyer 2011) as well as in the calculation of hydrodynamic properties with bead models (Byron 1997; Zipper & Durchschlag 1997; de la Torre *et al.* 2000). By construction, the N-particle mobility matrix obtained using (2.8) is positive definite and all the hydrodynamic tensors have the correct limiting behaviour for touching spheres and for complete overlap, with one sphere immersed in another.

Acknowledgements

P.J.Z. acknowledges support of the Foundation for Polish Science (FNP) through the TEAM 2010-6/2 project co-financed by the EU European Regional Development Fund.

E.W. and K.M. acknowledge the support of the Polish National Science Centre (grant no. 2012/05/B/ST8/03010). P.S. acknowledges the support of the Polish Ministry of Science and Higher Education (grant no. N N202 055440).

References

ANTOSIEWICZ, J. & PORSCHKE, D. 1989 Volume correction for bead model simulations of rotational friction coefficients of macromolecules. *J. Phys. Chem.* **93**, 5301–5305.

ARYA, G., ZHANG, Q. & SCHLICK, T. 2006 Flexible histone tails in a new mesoscopic oligonucleosome model. *Biophys. J.* **91**, 133–150.

BANACHOWICZ, E., GAPINSKI, J. & PATKOWSKI, A. 2000 Solution structure of biopolymers: a new method of constructing a bead model. *Biophys. J.* **78**, 70–78.

BLOOMFIELD, V., DALTON, W. O. & VAN HOLDE, K. E. 1967 Frictional coefficients of multisubunit structures. I. Theory. *Biopolymers* **5**, 135–148.

BYRON, O. 1997 Construction of hydrodynamic bead models from high-resolution X-ray crystallographic or nuclear magnetic resonance data. *Biophys. J.* **72**, 408–415.

CARRASCO, B. & DE LA TORRE, G. J. 1999 Hydrodynamic properties of rigid particles: comparison of different modeling and computational procedures. *Biophys. J.* **76**, 3044–3057.

CARRASCO, B., DE LA TORRE, J. G. & ZIPPER, P. 1999 Calculation of hydrodynamic properties of macromolecular bead models with overlapping spheres. *Eur. Biophys. J.* **28**, 510–515.

CICHOCKI, B., FELDERHOF, B. U., HINSEN, K., WAJNRYB, E. & BŁAWZDZIEWICZ, J. 1994 Friction and mobility of many spheres in Stokes flow. *J. Chem. Phys.* **100**, 3780–3790.

CICHOCKI, B., JONES, R. B., KUTTEH, R. & WAJNRYB, E. 2000 Friction and mobility for colloidal spheres in Stokes flow near a boundary: the multipole method and applications. *J. Chem. Phys.* **112**, 2548–2561.

CLEMENTI, C. 2008 Coarse-grained models of protein folding. *Curr. Opin. Struct. Biol.* **18**, 10–15.

DHONT, J. K. G. 1996 *An Introduction to Dynamics of Colloids*. Elsevier Science.

DŁUGOSZ, M., ZIELIŃSKI, P. & TRYLSKA, J. 2011 Brownian dynamics simulations on CPU and GPU with BD BOX. *J. Comput. Chem.* **32**, 2734–2744.

DUGUET, E., DÉSERT, A., PERRO, A. & RAVAINE, S. 2011 Design and elaboration of colloidal molecules: an overview. *Chem. Soc. Rev.* **40**, 941–960.

ERMAK, D. L. & MCCAMMON, J. A. 1978 Brownian dynamics with hydrodynamic interactions. *J. Chem. Phys.* **69**, 1352–1360.

FELDERHOF, B. U. & JONES, R. B. 1989 Displacement theorems for spherical solutions of the linear Navier–Stokes equations. *J. Math. Phys.* **30**, 339–342.

FREMBGEN-KESNER, T. & ELCOCK, A. H. 2009 Striking effects of hydrodynamic interactions on the simulated diffusion and folding of proteins. *J. Chem. Theory Comput.* **5**, 242–256.

GEYER, T. 2011 Many-particle Brownian and Langevin dynamics simulations with the Brownmove package. *BMC Biophys.* **4**, 7.

HELLWEG, T., EIMER, W., KRAHN, E., SCHNEIDER, K. & MÜLLER, A. 1997 Hydrodynamic properties of nitrogenase – the MoFe protein from *Azotobacter vinelandii* studied by dynamic light scattering and hydrodynamic modelling. *Biochem. Biophys. Acta* **1337**, 311–318.

HILLS, R. D. JR. & BROOKS, C. L. III 2009 Insights from coarse-grained Go models for protein folding and dynamics. *Intl J. Mol. Sci.* **10**, 889–905.

KIM, S. & KARRILA, S. J. 1991 *Microhydrodynamics: Principles and Selected Applications*. Butterworth-Heinemann.

KIRKWOOD, J. G. & RISEMAN, J. 1948 The intrinsic viscosities and diffusion constants of flexible macromolecules in solution. *J. Chem. Phys.* **16**, 565–573.

NÄGELE, G. 2006 Brownian dynamics simulations. In *Computational Condensed Matter Physics,* vol. B4:1 (ed. S. Blügel, G. Gompper, E. Koch, H. Müller-Krumbhaar, R. Spatschek & R. G. Winkler), Forschungszentrum Jülich.

ROTNE, J. & PRAGER, S. 1969 Variational treatment of hydrodynamic interaction in polymers. *J. Chem. Phys.* **50**, 4831–4837.

SZYMCZAK, P. & CIEPLAK, M. 2007 Proteins in a shear flow. *J. Chem. Phys.* **127**, 155106.

SZYMCZAK, P. & CIEPLAK, M. 2011 Hydrodynamic effects in proteins. *J. Phys.: Condens. Matter* **23**, 033102.

DE LA TORRE, J. G. & BLOOMFIELD, V. A. 1977 Hydrodynamic properties of macromolecular complexes. I. Translation. *Biopolymers* **16**, 1747–1763.

DE LA TORRE, G. J., HUERTAS, M. L. & CARRASCO, B. 2000 Calculation of hydrodynamic properties of globular proteins from their atomic-level structure. *Biophys. J.* **78**, 719–730.

TOZZINI, V. 2005 Coarse-grained models for proteins. *Curr. Opin. Struct. Biol.* **15** (2), 144–150.

WAJNRYB, E., MIZERSKI, K. A., ZUK, P. J. & SZYMCZAK, P. 2013 Generalization of the Rotne–Prager–Yamakawa mobility and shear disturbance tensors. *J. Fluid Mech.* **731**, R3.

WAJNRYB, E., SZYMCZAK, P. & CICHOCKI, B. 2004 Brownian dynamics: divergence of mobility tensor. *Physica* A **335**, 339–358.

ZIPPER, P. & DURCHSCHLAG, H. 1997 Calculation of hydrodynamic parameters of proteins from crystallographic data using multibody approaches. *Prog. Colloid. Polym. Sci.* **107**, 58–71.

ZURITA-GOTOR, M., BŁAWZDZIEWICZ, J. & WAJNRYB, E. 2007 Motion of a rod-like particle between parallel walls with application to suspension rheology. *J. Rheol.* **51**, 71–97.

ZWANZIG, R., KIEFER, J. & WEISS, G. H. 1968 On the validity of the Kirkwood–Riseman theory. *Proc. Natl Acad. Sci. USA* **60**, 381–386.